GOESR3 Final Report

Reporting Period: **July 2017 – June 2020 (full 3-year period)**

Team Lead: John M. Haynes
Team Members: Yoo-Jeong Noh, Steven D. Miller, Andrew Heidinger

Project Title: Improving the ABI Cloud Layers Product for Multiple Layer Cloud Systems and Aviation Forecast Applications

Project Number: 479

Executive Summary

We note that this work is currently continuing under a **no-cost extension**, so we are treating this report as a summary of the project and **important results to date**, and a **description of ongoing work during the extension**. We will then issue a short addendum at the end of the project to summarize new work.

This project seeks to improve the classification and categorization of multilayer cloud scenes by the GOES ABIs, while simultaneously improving the Cloud Cover Layers (CCL) product that identifies the height category of clouds in any given ABI pixel. The motivation for the project is the inherent difficulties in retrieving information about cloud vertical extent from passive instrument measurement(s), including those made by the ABI. Although it is often possible to determine the cloud top height (CTH) of the upper-most cloud layer, it is difficult to estimate the depth of the cloud from ABI measurements alone, and it is even more of a challenge to identify, let alone quantify, the height of underlying cloud layers. This challenge can be clarified by evaluating the performance of the CCL product using an independent dataset (for example, the spaceborne CloudSat radar and CALIPSO lidar; see Figure 1).

This project's goal was to *improve the classification and categorization of vertical cloud extent within a given ABI-observed scene.* The general methodology at the start of this work was threefold: (1) To investigate the usefulness of certain cloud proxies, such as layer relative humidity, by training on actively-sensed cloud layer boundaries; (2) To develop a new multispectral retrieval that uses ABI radiances to determine separation between cloud layers in known multilayer situations; and (3) To fuse this information together with our own statistical cloud base algorithm, which has been trained on radar and lidar-observed cloud boundaries.

Task (1) was completed during the course of the work, and Task (3), representing the final product, is ongoing during the no-cost extension. Task (2) transitioned during the course of the project from a lookup table approach using a radiative transfer model, into a machine learning based implementation of a new low cloud detection algorithm that we developed. Although fusion of Task (2) into a final product is ongoing, we have succeeded in bringing a new version of the CCL algorithm into the NOAA Enterprise Algorithm suite. This means that the new CCL algorithm is now an operations-ready component of the ABI algorithm suite.

Final Year Milestones (FY19) and Project Deliverables

This section contains on overview of our changes to the ABI CCL product, followed by a report on the first two tasks described above and their main outcomes during the course of the project. (The third task represents the fusion of the first two tasks, and is reported on in the following section dealing with operational transition.) This is followed by a report on auxiliary work we have done to create GOES-based cross sections of flight profiles for flight routes in the continental United States (CONUS). Finally, this section will highlight the FY19 milestones.

CCL V2 Product

During this project we have succeeded in bringing a new version of the CCL algorithm using cloud base height information (Noh et al. 2017) into the NOAA Enterprise Algorithm suite. This CCL algorithm (which we refer to as CCL V2 in this document) is now an operations-ready component of the ABI algorithm suite. The algorithm has been transformed from a simple algorithm with three height-based categories, high (H), middle (M), or low (L), which we refer to as the CCL V1 algorithm, to an algorithm with six categories (adding H+M, M+L, and H+M+L). An incremental minor improvement on top of this is that the algorithm can now be run on five flight-level based levels, a change that was made based on input from our operational partners with collaboration with Andy Heidinger (NOAA cloud team lead) and the CIMSS team. Figure 2 shows an example of the CCL V2 product, which can be viewed on CIRA's SLIDER tool (https://rammb-slider.cira.colostate.edu) where it is produced in near real-time. More details on transitions to operations can be found in the next section.

Task 1: Use of cloud proxies to locate low clouds missed by ABI

The purpose of this task was to explore the use of proxies for cloud cover, specifically relative humidity (RH) as determined from numerical weather prediction (NWP) models. To this end we completed an extensive study on the correlation between RH and the presence of clouds as viewed by two active sensors, the spaceborne CloudSat radar and CALIPSO lidar. The radar and lidar together are able to identify most clouds in their small footprint with low ambiguity. To accomplish this, we divided the globe into 5° x 5° boxes, accumulating cloud detections from the radar and lidar overpasses, and also recording information about the maximum RH in the column at the time of detection (the column is subdivided into several layers for this purpose). We used ECMWF forecast model RH, as it is been conveniently subset to the radar/lidar track and is available from the CloudSat Data Processing Center.

As covered in previous reports, we found that RH can serve as useful cloud proxy in the lowest layers of the atmosphere, but the utility is limited to certain regions of the globe, and also has a seasonal dependence. Figure 3 demonstrates some of these issues. The figure shows the hit rate (left column) and false alarm ratio (right column) of clouds correctly predicted in the 10–18 kft level by a RH threshold exceeding 70% (top row) and 90% (bottom row). The upper-left panel, for example, shows that over the CONUS more than 70% of the low clouds observed by radar/lidar are correctly predicted to occur if we assume that they are present anytime the RH in the layer is 70% of higher. The upper-right panel reveals that the association fraction of incorrect low cloud forecasts in this same region can exceed 50% using this method. By using a higher RH threshold (lower rows), we can reduce the false alarms, but at the expense of missed detections. Note also that while RH-based methods of cloud detection are feasible in the middle-latitude (over much of the CONUS, for example), the false alarms are much greater in the tropics. This is due to the presence of cloud-free moisture plumes in subsidence regions of the tropical atmosphere.

The chief finds of this portion of the study were that RH can be a useful predictor of low cloud in a way that is regionally and seasonally dependent, but RH cannot be used as a "drop in" proxy for cloud cover in most cases. This led us to search for ways to incorporate RH into our proxy, without using hard thresholds; and this brings us to chief results from Task 2.

Task 2: Multi-spectral / RH based retrieval of low clouds missed by ABI

As noted above, Task 2 transitioned from a physically based multi-spectral retrieval using a lookup table approach into a machine learning (ML) low cloud detection problem. While still using a variety of multispectral ABI information as originally proposed, we have shifted our focus to ML to more effectively merge these data with the non-linear characteristics on multilayer cloud scenes, training an algorithm that places clouds vertically in a scene utilizing training observations derived from the CloudSat radar and CALIPSO lidar. The driving factor for this change was the discovery that RH information is valuable for locating low clouds, especially under higher cloud layers, but hard thresholds are difficult to implement algorithmically. We also wished to use information from more channels than the initially proposed methodology allowed. This led us to develop a ML-based algorithm that takes multispectral information from the ABI, as well as vertical profiles of RH from NWP, and uses this information to directly predict the presence of a low-level cloud in the column. This algorithm is also applicable to other sensors, including VIIRS (with minor changes necessary to account for channel differences).

Our ML algorithm uses multiple ABI channels and external humidity profiles from the ECMWF model (the choice of model can easily be tailored to the type of NWP information available). For the results that follow, we used 35 days of parallax-corrected matched ABI/CloudSat/CALIPSO data (about 1.7 million data points) from 2017 in the latitude band of 60°N– 60°S. (The number of datapoints has since been expanded, with minimal impact on the results.) For each training data point, we evaluated the "truth" about the presence of low cloud from co-located CloudSat radar and CALIPSO lidar observations. Two versions of the algorithm were developed, one for daytime and one for night (the latter, and the fusion between the two algorithms, is part of the active development during the no-cost extension). The inputs to the ML model have been determined by a combination of physical relevance to the low cloud detection problem, and information content analysis that is produced by the algorithm itself. The daytime algorithm uses the following as predictors:

- ABI channels 1–3, 7, 10, 14 (0.47, 0.64, 0.87, 3.9, 7.34, 11.2 μm)
- TB 10.35 μm – TB 12.3 μm
- TB 3.9 μm – TB 11.2 μm
- 1.38 / 0.64 μm reflectance ratio
- NWP profiles of relative humidity in 0–1.9, 1.8–4, 4–6.2 km layer
- Solar zenith angle
- Latitude

The nighttime algorithm is different only in the channels used; in particular, inputs containing channels with wavelengths less than 3.9 μm are eliminated. Although not shown in the included figures, we have also added a surface characterization flag based on microwave-derived data from the National Snow and Ice Data Center as a predictor. This optional predictor increases overall accuracy by about 1–2%.

The Random Forest classifier model was used, which is an ensemble decision tree algorithm (Breiman 2001). During training, a number of decision trees are developed (a forest), each using a random subset of the training features. This reduces variance error and overfitting while minimizing bias error. During prediction, each tree in the forest comes to a low cloud "yes" or "no" conclusion based on its unique combination of inputs. After each tree comes to a decision, a group vote determines the final determination of cloud presence.

The performance of the daytime CCL V3 algorithm on an independent test data set is show in Figure 4. In this mode, the low cloud prediction by the ML model is used to supplement the original prediction by CCL V2 (i.e. if CCL V2 predicts no low cloud, but the ML model determines that low cloud is present for a pixel, then cloud is added into the column). The left panel shows the probability of detection (POD) of low cloud as a function of CLAVR-x cloud type in the test data set; the right panel shows the corresponding false alarm ratio (FAR). Bars are the new CCL V3, and asterisks are CCL V2.

What we immediately can immediately determine from this figure is that the new algorithm produces an overall improvement in the POD for low cloud in all categories (0.95 vs. 0.79), with only a slighter higher FAR (0.22 vs. 0.19). The differences are most dramatic for those cloud categories that contain the most overlapping cloud layers, such as “Overlapping” and “Cirrus”. In the cirrus category, for example, the POD increases to 0.69 from 0.22. This comes at the expense of a higher number of false alarms, but the false alarm rate for low cloud under cirrus is less than 25%, and during the extension period we are working to reduce this number by using more training data and improved characterization of the earth’s surface. The conditional success index (CSI; not shown) for CCL V3, which attempts to combine the offsetting effects of POD and FAR, is greater than or equal to that of CCL V2 for all cloud categories, showing an across-the-board improvement in low cloud detection. The nighttime algorithm suffers some degradation compared to the daytime algorithm, with POD about 4% lower and FAR about 10% higher.

An example full disk run of the new algorithm, and comparison against the previous algorithm, is shown in Figure 5. The most significant change is the shifting of clouds from the H+M category to the H+M+L category, which is especially apparent in the deepest parts of the tropical cyclone and frontal system apparent in the top of the image (in the North Atlantic).

Product Demonstration for Aviation Applications

In addition to our promised deliverables, the CIRA team has been supporting the VIIRS cloud product demonstration for Alaska users as part of the JPSS Aviation Initiative efforts. We developed cloud vertical cross-section products along flight routes by combining cloud top and base heights and cloud phase retrievals to provide satellite-based information on cloud vertical layers which has been a main interest in the aviation community. Temperature data and PIREPs (turbulence and icing) for selected flight routes were also added based on user feedback. With the success of this effort among aviation users in Alaska, the results were presented at 2020 JPSS/GOES-R PGRR Summit last February, and we received a request from NWS people working in the west coast region to extend the product generation to CONUS. Leveraging the JPSS VIIRS research, we developed the CONUS aviation website and started providing the cloud vertical cross-section products from GOES-16 ABI along selected flight routes for eight major airports. PIREPs within 30 miles and one hour along the routes were also displayed with the freezing level (from GFS). Figure 6 shows an example. These products from GOES-16 ABI (currently hourly data) together with JPSS VIIRS over CONUS are available in near real-time at http://rammb.cira.colostate.edu/ramsdis/online/npp_viirs_conus_aviation.asp.

Comments on Year 3 Milestones

• *Extensively test and validate algorithm using CloudSat, CALIPSO, EarthCare, and ARM data, as availability allows.*

CloudSat and CALIPSO data have been our main source of data, being used extensively for both algorithm development (training) and testing, as described above. EarthCare has not yet launched.

In addition, Danya Elliott (undergrad, Mechanical Engineering/CSU) joined as a CIRA summer intern student for CBH/CCL product evaluation, at no cost to the project. She compiled Department of Energy Atmospheric Radiation Measurement (ARM) surface measurements (Ceilometer and Micro-Pulse Lidar data) from NSA/Alaska and SGP/Oklahoma sites (2018-2020) and collected multilayer cases by comparing collocated CALIPSO and CloudSat (upon data availability) for validation which we plan to use for case studies in a journal paper. Sample ground lidar data for cloud top and base heights selected from 2019 matchups are shown in Figure 7.

• *Complete implementation of new algorithm into the CLAVR-x processing system (as a development/transition tool for NOAA operational algorithms).*

CCL V2 algorithm is part of the NOAA Enterprise Algorithm suite. We are working on CCL V3 during the no-cost extension. See the next section.

• *Complete incorporation and display test of the product in AWIPS II or NAWIPS.*

An implementation has been developed. See the next section.

• *Complete VISIT module training module for AWC forecasters.*

We developed user quick guides that users can obtain brief descriptions on the cloud base and vertical layer products, leveraging the JPSS cloud research at CIRA. The documents are available at http://rammb.cira.colostate.edu/training/visit/quick_guides/QuickGuide_JPSS_VIIRS_CBH.pdf and http://rammb.cira.colostate.edu/ramsdis/online/product_info/quickguide_jpss_viirs_cvc_cira.pdf, which were initially developed with VIIRS but also applicable to GOES0-16 and -17 ABIs. During the no-cost extension period we are working with VISIT to update the current materials and develop for forecaster-oriented training tools extended for our new satellite product using machine learning.

• *Visit Aviation Weather Center to deliver hands on training.*

John Haynes visited the Aviation Weather Center in August 2019 to gather user feedback and interact with forecasters. The COVID-19 public health crisis prevented a follow-up trip from happening, and it is unclear at this time when such a trip might be possible. Even so, we have remained in frequent contact with our AWC partners.

• *Present results at GOES-R meeting and at AMS or AGU.*

A much more thorough list of presentation can be found in the "Additional Information" section below; the following two items are meant only to address this particular milestone. This work was presented in an oral presentation at the American Meteorological Society / EUMETSAT Joint Satellite Conference in Boston, Massachusetts and at the JPSS/GOES-R Proving Ground Risk Reduction Summit in College Park, Maryland.

Noh, Y. J., S. D. Miller, J. M. Haynes, J. M. Forsythe, C. J. Seaman, A. Heidinger, A. Walther, Y. Li, W. Straka, 2020: Cloud Base and Cloud Cover/Layers. JPSS/GOES-R Proving Ground Risk Reduction Summit, February 24-28, 2020, College Park, MD.

Haynes, J. M., Y. J. Noh, S. D. Miller, A. K. Heidinger, and J. M. Forsythe, 2019: Cloud boundary detection in multilayer scenes with the GOES ABI. 2019 American Meteorological Society / EUMETSAT Joint Satellite Conference, 28 September - 4 October 2019, Boston, MA.

• *Publish results in a journal.*

This is a major focus at present. We are preparing this work now, with the working title *Cloud boundary detection in multilayer scenes with the GOES ABI.*

Discussion of operational transition readiness for any project outcomes

CCL V2 Product: Operational Transition and N-AWIPS Interface

As noted above, we have succeeded in bringing the CCL V2 algorithm into the NOAA Enterprise Algorithm suite. In August 2019, PI John Haynes visited the AWC in Kansas City, MO. He updated staff on our CCL work, garnered user feedback, and interacted with forecasters on the operations floor. Gathering user feedback on how satellite cloud products are used by AWC forecasters was invaluable, providing a better understanding of user needs for low-cloud products, and how our CCL benefits AWC forecasters, particularly in the arena of general aviation forecasting. The machine-learning approach we have embraced in the V3 algorithm was well received. This visit resulted in development of an N-AWIPS interface for operational forecasters. An example of this interface is show in Figure 8. The display shows clouds layer combinations in a variety of colors, comparable to the SLIDER we use for product testing and public dissemination. We have determined the steps required to deliver this product AWC via LDM, and planned to coordinate this (and perform additional training) during a trip to AWC in the first half of 2020; unfortunately, however, the public health crisis slowed this progress. We will instead discuss these next steps during the no-cost extension period.

CCL V3 Product: A Post-processing routine for CLAVR-x

As noted in the previous section, the CCL V3 product is under active development during the no-cost extension. We are currently developing the code as a post-processing routine for CLAVR-x. The reason for this is that it eliminates the extremely time-intensive step of developing a Fortran implementation of Random Forest, particularly one that is compatible with the model training routines we utilize (nearly all modern ML implementations are in Python, not Fortran). It is also convenient that CCL V3 can be run as a post-processing routine, running only on CLAVR-x output (with some minor modifications, such as inclusion of NWP-based relative humidity in layers). It can be configured in two modes, (1) to insert low cloud as a supplement to our CCL V2 determination, or (2) to replace the CCL V2 low cloud determination completely. During the extension, we will extensively test both methods, implementing the algorithm into our SLIDER testbed, and working to better incorporate it into the workflow of the Enterprise Algorithms (using simple scripts, or direct calls to Python from the Fortran interface itself depending on its computational cost and processing time).

Additional Information

1. Interaction with operational partners –

Multiple interactions with Aviation Weather Center, as described throughout this document, including one physical visit and assistance/input on N-AWIPS development.

Leveraging the JPSS cloud research at CIRA, we have been participating in the Aviation Initiative, interacting with Alaska operational users (NWS Alaska Aviation Weather Unit and Aviation Testbed) and pilots. User feedback through user-developer interactions on satellite-based cloud vertical layer information that we are providing has been incorporated in algorithm improvement, training materials for users, and product display.

2. Conference/workshop participation –

Y. J. Noh attended the Artificial Intelligence for Earth System Science (AI4ESS) Summer School (June 22-26, 2020), which were virtually held (no cost to project) and hosted by NCAR.

Haynes, J. M., Y. J. Noh, S. D. Miller, and A. K. Heidinger, 2020: Cloud Boundaries and Low Cloud Detection for the GOES ABI Trained with CloudSat/CALIPSO Data. 2020 CloudSat/CALIPSO Annual Science Review, Boulder, CO.

Noh, Y. J., S. D. Miller, J. M. Haynes, J. M. Forsythe, C. J. Seaman, A. Heidinger, A. Walther, Y. Li, W. Straka, 2020: Cloud Base and Cloud Cover/Layers. JPSS/GOES-R Proving Ground Risk Reduction Summit, February 24-28, 2020, College Park, MD.

Noh, Y. J., S. D. Miller, J. M. Haynes, J. M. Forsythe, C. J. Seaman, J. Kim, and A. Heidinger, 2020:

Satellite Cloud Vertical Cross-section Products and User-Engaged Improvement for Aviation Weather Applications. 100th AMS Annual Meeting/20th Conference on Aviation, Range, and Aerospace Meteorology, January 12-15, 2020, Boston, MA.

Haynes, J. M., Y. J. Noh, S. D. Miller, A. Heidinger, and J. M. Forsythe, 2019: Cloud geometric thickness and improved cloud boundary detection with the GOES ABI. 15th Annual Symposium on New Generation Operational Environmental Satellite Systems, American Meteorological Society 99th Annual Meeting, Phoenix, Arizona.

Noh, Y. J., S. D. Miller, J. M. Haynes, J. M. Forsythe, C. J. Seaman, A. Heidinger, and Y. Li, 2019: Improvement of nocturnal cloud base height and vertical layer retrievals in high latitudes, 99th AMS Annual Meeting/15th Annual Symposium on New Generation Operational Environmental Satellite Systems, 6-10 January 2019, Phoenix, AZ (Oral presentation at Session on Nighttime Environmental Monitoring)

Noh, Y. J, S. Miller, J. Haynes, J. Forsythe, C. Seaman, A. Heidinger, A. Walther, Y. Li, S. Wanzong, and W. Straka, 2019: Satellite Cloud Base/Layer Product and Aviation Weather Applications. 4th KNU CARE International Conference, Sept. 23-24, 2019, Gyeongju, Korea. (Invited talk).

Noh, Y. J., J.-H. Kim, S. D. Miller, 2019: Satellite Cloud Vertical Layers for Aviation Weather Applications. 2019 Korean Meteorological Soc. Annual Fall Meeting, Oct. 30 – Nov. 1, 2019, Gyeongju, South Korea.

Haynes, J. M., Y. J. Noh, S. D. Miller, A. K. Heidinger, and J. M. Forsythe, 2019: Cloud boundary detection in multilayer scenes with the GOES ABI. 2019 American Meteorological Society / EUMETSAT Joint Satellite Conference, 28 September - 4 October 2019, Boston, MA.

Noh, Y. J., S. D. Miller, J. M. Haynes, J. M. Forsythe, C. J. Seaman, A. Heidinger, A. Walther, and Y. Li, 2019: Improvement of Nighttime Cloud Geometric Thickness Retrieval Integrating Multi-Sensor Observations and Numerical Model Simulations. 2019 AMS-EUMETSAT Joint Satellite Conference. 28 September - 4 October 2019, Boston, MA.

Noh, Y. J., 2019: CIRA's satellite products, COMET Weather Analysis and Forecasting course for Korea Meteorological Administration forecasters. 14 May 2019, Boulder, CO.

Miller, S. D., Y.-J. Noh, D. T. Lindsey, C. J. Seaman, J. M. Forsythe, J. M. Haynes, and L. D. Grasso, 2018: Aviation-Relevant Satellite Research and Algorithm Development at CIRA. FAA Aviation Weather Research Program (AWRP) Review Meeting, 10-11 July, Boulder, CO. (Invited talk)

Miller, S. D., C. J. Seaman, Y.-J. Noh, D. T. Lindsey, J. M. Forsythe, J. F. Dostalek, J. R. Torres, and K. P. Micke, 2018: CIRA Development of Alaska-Relevant Satellite Applications from Suomi-NPP, JPSS-1 and GOES-R. ACCAP Virtual Alaska Weather Symposium, 22 August 2018.

3. Outside project publicity –

None.

4. Journal articles –

This is a major focus during the no-cost extension period. We are preparing this work now, with the working title *Cloud boundary detection in multilayer scenes with the GOES ABI using machine learning.*

5. References used in this report –

Breiman, L., 2001: Random forests. *Mach. Learn.*, **45**, 5–32, https://doi.org/10.1023/A:1010933404324.

Noh, Y.-J., and Coauthors, 2017: Cloud-base height estimation from VIIRS. Part II: A statistical algorithm based on A-Train satellite data. *J. Atmospheric Ocean. Technol.*, **34**, 585–598, https://doi.org/10.1175/JTECH-D-16-0110.1.

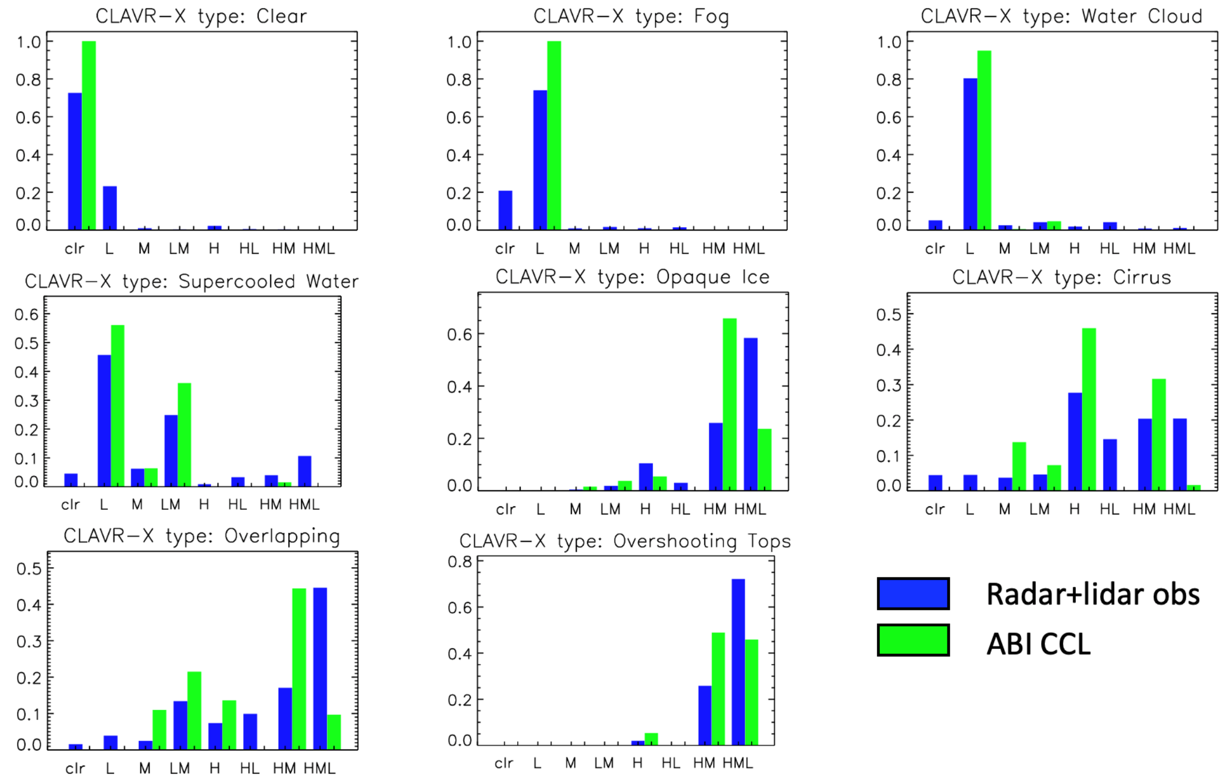

Figure 1. Cloud statistics for eight different CLAVR-x categories showing statistics of joint observations between GOES-16 ABI, CloudSat, and CALIPSO (each panel represents one such category). The vertical axis of each panel is the fraction of observed cases during the test period. The horizontal axis shows the vertical height categories. Blue bars are radar+lidar observations, green bars are ABI using the CCL V2 algorithm.

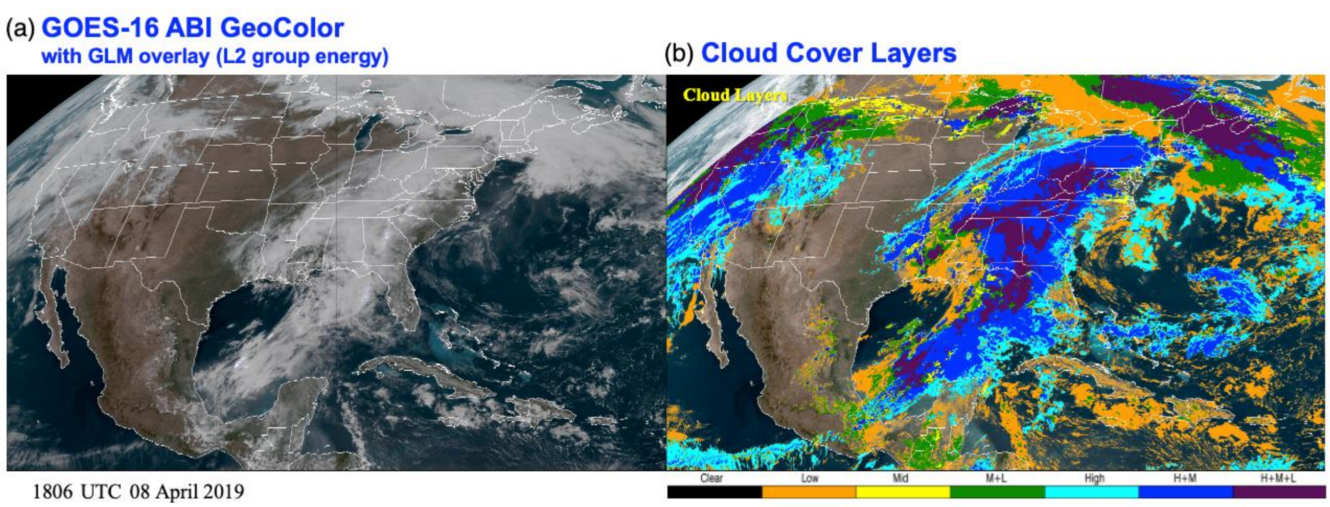

Figure 2. Sample GOES-16 (a) GeoColor image with GML overlay, and (b) CCL depiction at 08 April 2019 18:06 UTC. Cloud Cover Layers and Cloud Geometric Thickness products are currently being displayed in CIRA's SLIDER (https://rammb-slider.cira.colostate.edu) with other cloud retrieval products and imagery for both GOES-16 and GOES-17 ABI for all four sectors in real time.

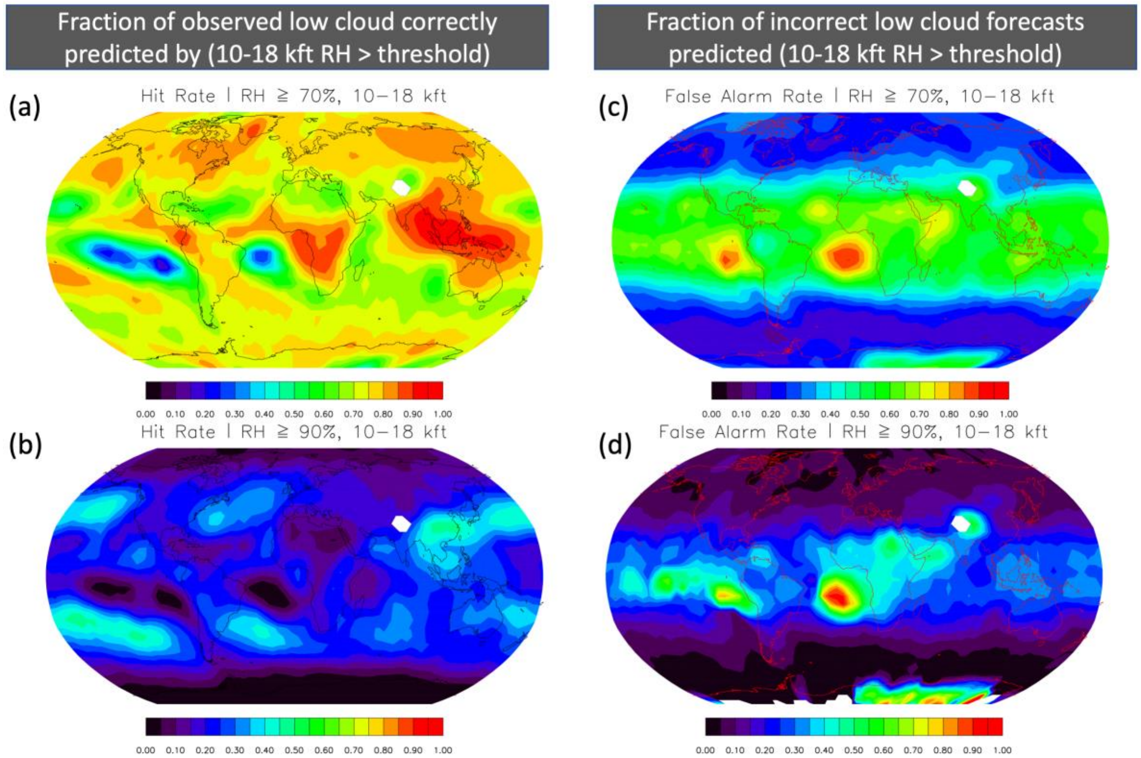

Figure 3. Hit rate (a,b) and false alarm ratio (c,d) of clouds correctly predicted in the 10-18 kft level by a RH threshold exceeding 70% (top row) and 90% (bottom row).

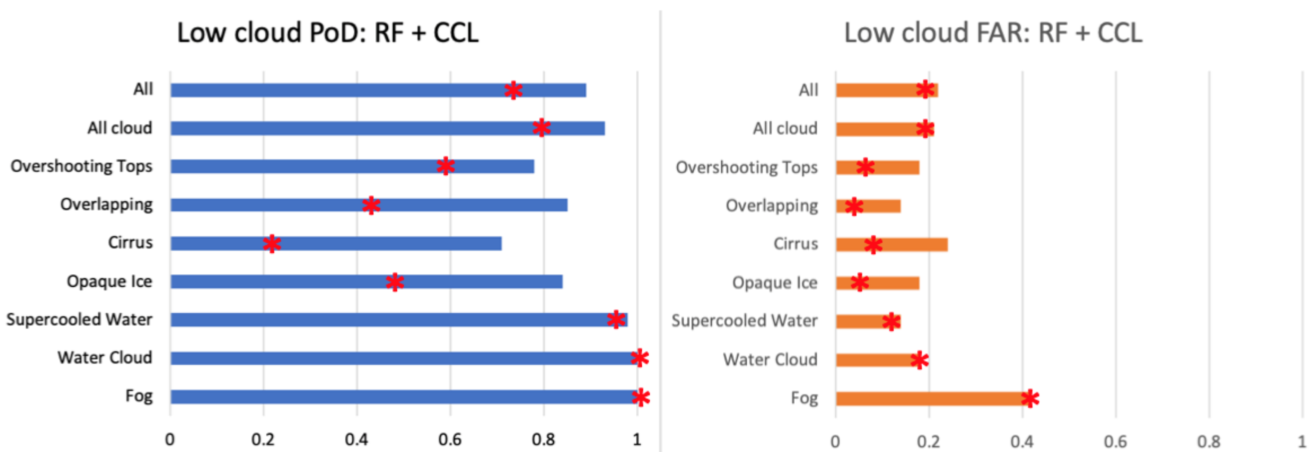

Figure 4. CCL V3 algorithm performance. Probability of detection (PoD; left panel) and false alarm ratio (FAR, right panel) of low cloud detection, as a function of CLAVR-x cloud type (labels on vertical axis). The bars represent either the PoD or FAR of an algorithm that classifies low cloud as occurring whenever the CCL algorithm detects low cloud OR the random forest implementation detects low cloud. The red asterisks represent the CCL V2 algorithm.

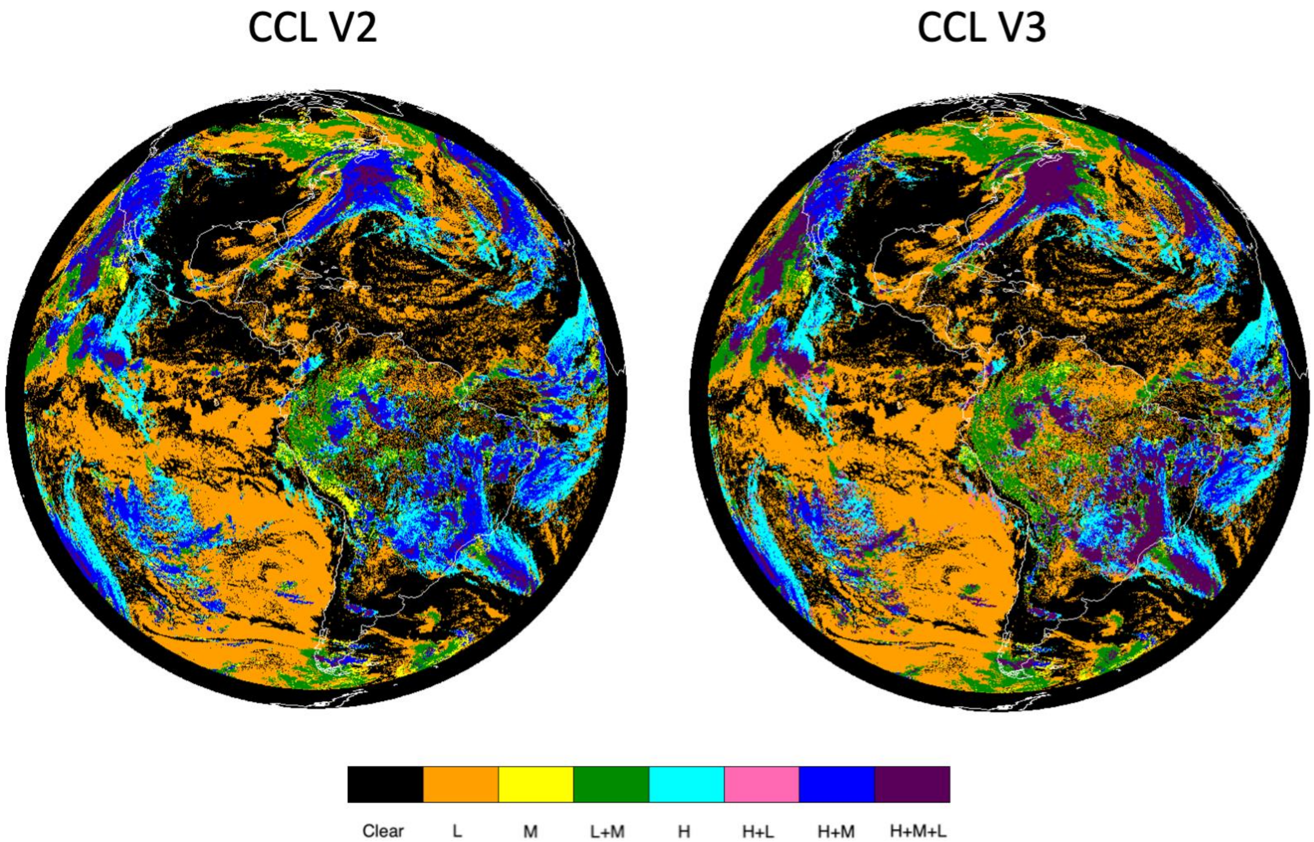

Figure 5. CCL V2 and CCL V3 algorithm results for a GOES-16 full disk image at 2019/01/05 17:15 UTC. Note that many H+M pixels (blue) in V2 are now categorized as H+M+L (violet) with increased L in V3 as well as new H+L (pink) appearance around deep convection, which was largely H only in V2.

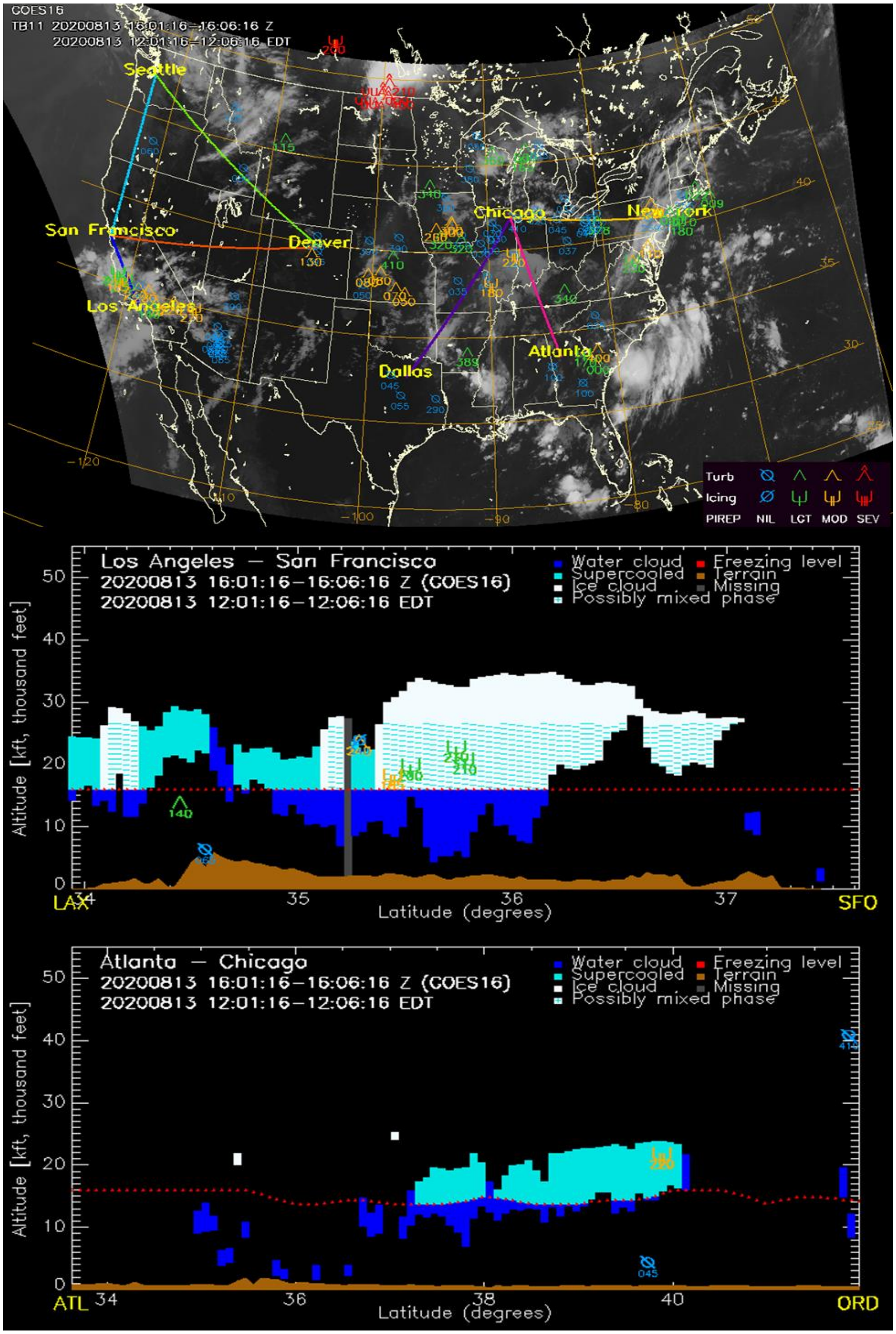

Figure 6. CIRA's cloud vertical cross-section products over CONUS for aviation users. Sample IR image of GOES-16 ABI 11.2 µm (top) and two cross-sections with PIREPs (icing and turbulence in ± 1 hour) along flight routes between Los Angeles and San Francisco (middle) and between Atlanta and Chicago (bottom). These products from JPSS VIIRS and GOES-16 ABI (hourly) are available at http://rammb.cira.colostate.edu/ramsdis/online/npp_viirs_conus_aviation.asp.

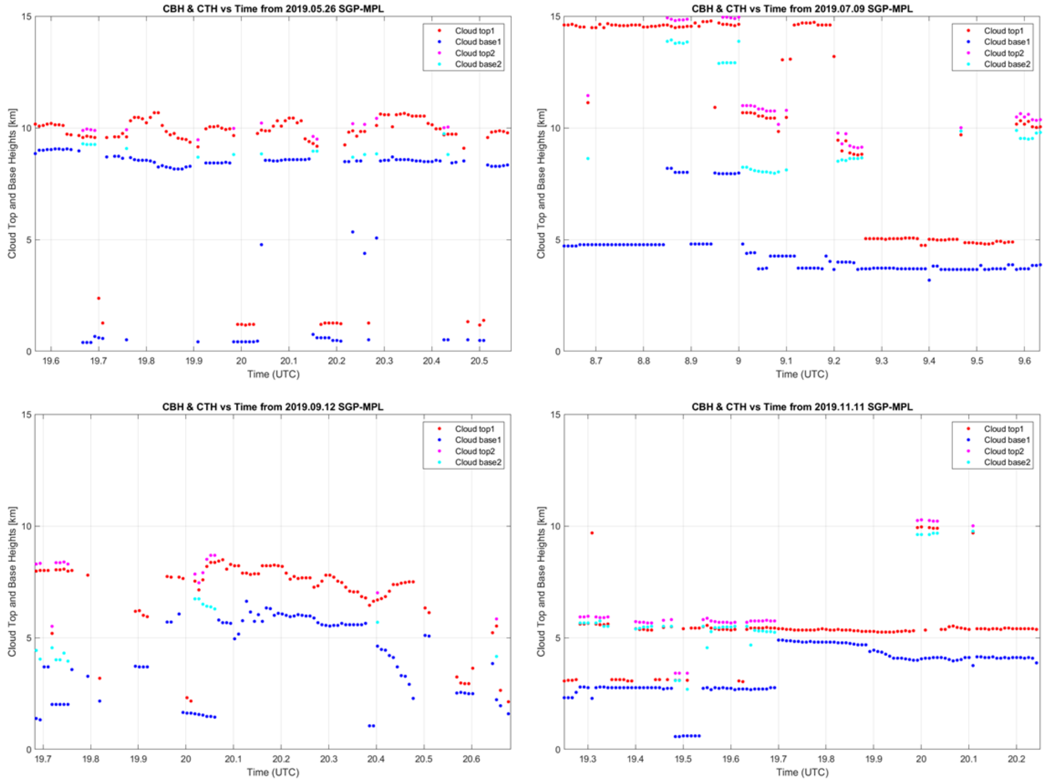

Figure 7. Sample cloud top (red/pink) and base (blue/cyan) height measurements from the Micro-Pulse Lidar (MPL) for selected multilayer cloud cases at the Atmospheric Radiation Measurement (ARM) Southern Great Plains (SGP) site in Oklahoma.

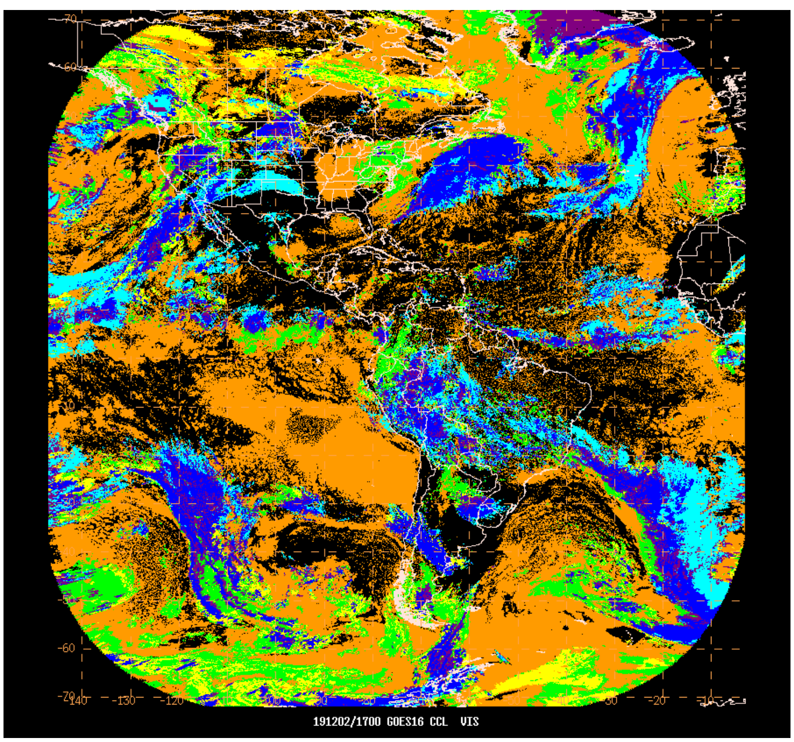

Figure 8. Initial test version of an N-AWIPS product display for CCL. Colors represent different combination of high (H), mid (M), and low (L) cloud layers, using the same scheme as Figure 2.